

Feature article:

Effects of finite chain extensibility on segmental orientation and stress in biaxially deformed polymers ^a

Leszek Jarecki*, Andrzej Ziabicki

Institute of Fundamental Technological Research, Polish Academy of Sciences, Swietokrzyska 21, 00-049 Warsaw, Poland; Fax (+48-22) 826-98-15; ljarecki@ippt.gov.pl; aziab@ippt.gov.pl

(Received: February 1, 2002; published: April 24, 2002)

Abstract: Development of biaxial segmental orientation and stresses in flexible chain polymers subjected to affine deformation of end-to-end vectors or to steady biaxial extensional flow is discussed. A closed-formula theory with non-Gaussian chain statistics and a Padè approximation of the inverse Langevin function is considered. The approach accounts for finite chain extensibility and is free from the problems of weak convergence of series-expansion expressions at higher molecular deformations. Average orientation tensor, global anisotropy tensor, and axial orientation factors characterise segmental orientation. Axial orientation factors and normal stress differences, in the deformation and normal planes, are discussed for biaxial affine deformation and steady biaxial elongational flow in a wide range of molecular deformations using inverse Langevin chain statistics. Orientation characteristics predicted for biaxial flow deformation are higher, and change in a wider range, than those in affine biaxial stretch. Also sensitivity to transversal deformation is different in both types of deformation.

Introduction

Mechanical and physical properties of polymers are strongly influenced by molecular orientation and its symmetry. Deformation of flexible-chain polymer systems during processing leads to orientation of individual chain segments, affects free energy and stresses. High modulus and tenacity of polymer fibres are consequences of high segmental orientation produced during the formation processes [1,2]. Molecular orientation influences also thermodynamic properties, related phase transition points and kinetics of crystallisation, as well as the crystalline morphology.

Increasing interest in obtaining high-performance films has led several authors to experimental [3-11] and theoretical [3,5,8,12-14] investigations on the development and characterisation of biaxial orientation. Aspects of the interest concern intramolecular as well as supramolecular constitution. Intramolecular, short range constitution, and related interactions, determine chain flexibility (rigidity). Aspects of supramolecular constitution concern the role of entanglements, viscoelasticity, physical or chemical crosslinking, etc. We concentrate here on flexible chain polymers and the

^a Presented at the Workshop on Polymers Dynamics, organized as part of the Excellence Centre of the European Commission in Lodz, Poland, November 15, 2001.

Related publications: Jarecki, L.; Ziabicki, A.; Polymer 2002, 43, 2549, 4063.

development of segmental orientation in solid and liquid state subjected to deformation of biaxial symmetry. Inverse Langevin chain statistics is used to describe the non-linear effects.

In the range of high biaxial (or uniaxial) molecular deformations, theoretical modelling of the development of segmental orientation in flexible chain systems should account for finite chain extensibility and non-Gaussian chain statistics. Such an analysis is much limited by the weak convergence of series expansion procedures used for non-Gaussian systems at higher deformations. This makes the series expansion approach difficult, or intractable, in the case of high molecular deformations for biaxial [13] or more complex deformation geometries.

In this presentation we discuss a closed-formula approach to biaxial orientation based on a Padè approximation of the inverse Langevin function [15]. We consider a system composed of monodisperse, freely jointed chain molecules with inverse Langevin distribution of the end-to-end vectors, subjected to biaxial deformation. Thermodynamic characteristics, molecular orientation, and stresses produced in the deformation may be used for predicting physical properties, crystallization kinetics and texture development.

In a solid state, the segmental orientation produced by cold or hot drawing, thermoforming, etc. is controlled first of all by deformation applied to the material. Orientation relaxation during processing is much reduced due to stresses transmitted directly to the chain ends in the case of crosslinked systems, or strong viscous friction in the case of uncrosslinked solids. Crosslinked, rubbery materials show reversible deformation, the extent of which can be correlated with the average segmental orientation. In uncrosslinked solids, strong interactions between polymer chains lead to plastic behaviour, with irreversible deformation and frozen orientation maintained long after the deformation stresses are released to zero. We assume affine deformation of the chain end-to-end vectors in the solid state.

In the fluid state, applied techniques such as film blowing or film casting yield segmental orientations controlled first of all by the deformation rate, or stress, in the case of purely viscous fluids. In more complex, viscoelastic materials, the effects of deformation and deformation rate superimpose. We assume that the viscous fluid is subjected to isochoric biaxial stretching flow which results in potential control of segmental orientation. Steady-state flow orientation is discussed.

In the following sections, segmental orientation and stress in an individual flexible chain, and their system averages in polymer solids subjected to biaxial affine deformation and in polymer fluids under steady-state biaxial elongational flow are discussed.

Segmental orientation and stress in an individual chain

Segmental orientation in an individual flexible chain is controlled by the applied stresses. The elastic free energy of a flexible chain with end-to end vector \mathbf{h} depends on the current chain extension h/Na and is represented by [16]

$$F_{el}(h) = NkT \int_0^{h/Na} L^*(x) dx \quad (1)$$

where h is the end-to-end distance, N the number of statistical Kuhn segments in the chain, a the statistical segment length, T the temperature, and k the Boltzmann constant.

The chain free energy is proportional to the inverse Langevin function $L^*(x)$ integrated between zero and h/Na . Eq. (1) is valid in the entire range of chain extension h/Na between zero and unity, and F_{el} depends parametrically on the number of chain segments, N .

The chain elastic potential F_{el} controls an elastic force acting between the chain ends

$$f = \nabla F_{el} = \frac{kT}{a} L^*(h/Na) \quad (2)$$

The elastic force is a non-linear function of the chain extension h/Na .

Orientation distribution of the statistical segments around the chain end-to-end vector \mathbf{h} shows cylindrical symmetry, and is expressed by a function of cosine of the angle α between a segment and the vector \mathbf{h} [17]

$$w_s(\cos \alpha) = \frac{L^*(h/Na)}{4\pi \operatorname{sh}[L^*(h/Na)]} \exp\left[L^*\left(\frac{h}{Na}\right) \cos \alpha\right] \quad (3)$$

The distribution depends parametrically on the actual chain extension h/Na .

The exact analytic formula of the inverse Langevin function $L^*(x)$ used for the chain elastic free energy, elastic force, and segmental orientation distribution is unknown. A series expansion approximation of $L^*(x)$ reads

$$L^*(x) = 3x + \frac{9}{5}x^3 + \frac{297}{175}x^5 + \frac{1539}{875}x^7 + \frac{126117}{67375}x^9 + \dots \quad (4)$$

but the expansion is slowly convergent at $x > 1/2$.

An approximation of $L^*(x)$ by the first term of series (4) leads to the Gaussian elastic free energy and corresponding orientation distribution. The approximation can be used for small chain extensions. At higher chain extensions, at $h/Na > 1/2$, the series-expansion approach is weakly convergent, and its application is ineffective [18].

Cohen [15] proposed a closed-formula Padè approximation of $L^*(x)$, satisfactorily good in the entire range of chain extensions

$$L^*(x) \cong x \frac{3 - x^2}{1 - x^2} \quad (5)$$

Exact plots of the inverse Langevin function, and its Padè (Eq. (5)) and Gaussian approximations are illustrated in Fig. 1. The plot of $L^*(x)$ represents the relation of the reduced elastic force fa/kT vs. chain extension h/Na (cf. Eq. (2)). The Gaussian approximation deviates significantly at $h/Na > 1/2$ and shows unphysical behaviour, i.e., finite elastic force at full chain extension. The Padè approximation shows minor deviations, slightly exceeding the exact plot at higher chain extensions. It converges asymptotically to $1/(1-x)$ at x approaching unity, and to $3x$ at small values of x .

The elastic force acting between the chain ends and the orientation distribution of statistical segments can be represented by tensorial characteristics assigned to the chain extension h/Na and to the end-to-end vector \mathbf{h} . The "local" molecular stress tensor is given by the tensorial product of the elastic force vector and the vector \mathbf{h} [19,20]:

$$\mathbf{p}(\mathbf{h}) = \frac{1}{Nv_0} \mathbf{f} \otimes \mathbf{h} = \frac{kT}{v_0} \left(\frac{h}{Na}\right) L^*\left(\frac{h}{Na}\right) \frac{\mathbf{h} \otimes \mathbf{h}}{h^2} \quad (6)$$

where v_0 denotes the volume per statistical segment in the system. The local stress corresponds to the elastic force acting between the ends of a non-Hookean elastic dumbbell, representing each chain.

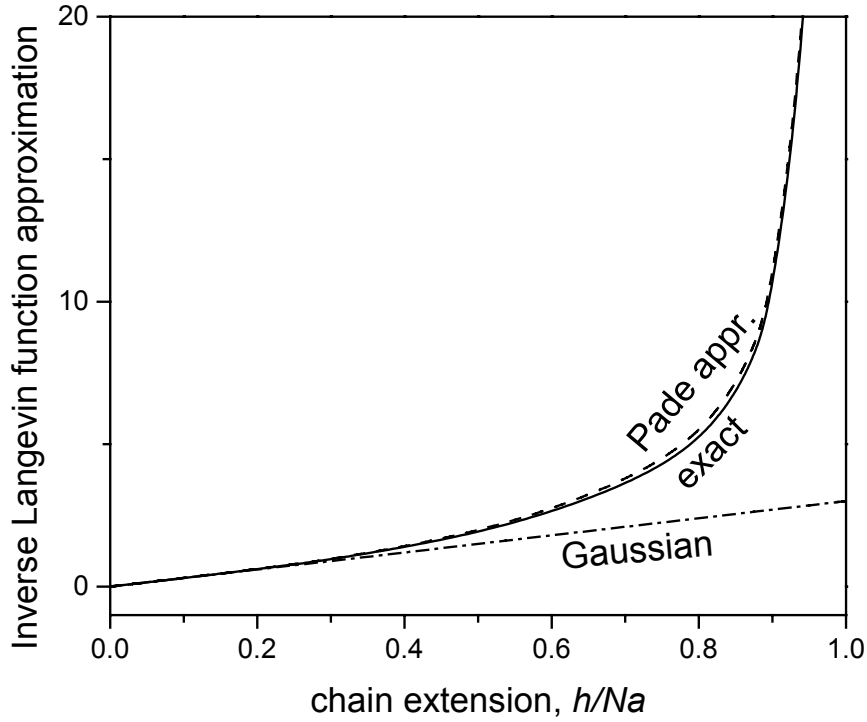


Fig. 1. Inverse Langevin function $L^*(h/NI)$ (exact, solid line); Padè approximation (dashed line); Gaussian approximation (dash-dotted line)

Orientation of the segments in an individual chain is given by the orientation tensor proposed by Zimm [17]

$$\mathbf{A}(\mathbf{h}) = \left[1 - \frac{3 \frac{h}{Na}}{L^*\left(\frac{h}{Na}\right)} \right] \frac{\mathbf{h} \otimes \mathbf{h}}{h^2} \quad (7)$$

At full chain extension, $h/NI = 1$, the function $L^*(h/NI)$ tends to infinity and the stress tensor \mathbf{p} diverges, while the segmental orientation tensor \mathbf{A} approaches $\mathbf{h} \otimes \mathbf{h}/h^2$, a form typical of a slim rigid rod of length h . This indicates that finite chain extensibility is the source of non-linearity of the stress-orientation behaviour at higher chain deformations. At zero chain extension, both tensors reduce to zero.

Eqs. (4), (6) and (7) lead to a non-linear stress-orientation relation for the individual chain in the form of a power series of the dimensionless stress $\mathbf{p}v_0/kT$

$$\mathbf{A}(\mathbf{p}) = \frac{1}{5} \frac{\mathbf{p}v_0}{kT} - \frac{3}{175} \left(\frac{\mathbf{p}v_0}{kT} \right)^2 - \frac{1}{875} \left(\frac{\mathbf{p}v_0}{kT} \right)^3 + \frac{13}{67375} \left(\frac{\mathbf{p}v_0}{kT} \right)^4 + \dots \quad (8)$$

At small stresses, the above series reduces to the well known linear stress-orientation law given by the first term, valid for Gaussian chain statistics. At higher stresses, the non-linear terms play a substantial role, and finite chain extensibility should be considered.

With the Padè approximation, the elastic free energy, stress, and orientation tensors of an individual chain read

$$F_{el}(h) \cong NkT \left\{ \frac{1}{2} \left(\frac{h}{Na} \right)^2 - \ln \left[1 - \left(\frac{h}{Na} \right)^2 \right] \right\} \quad (9)$$

$$\mathbf{p}(\mathbf{h}) \equiv \frac{kT}{v_0} \left(\frac{h}{Na} \right)^2 \left[\frac{3 - \left(\frac{h}{Na} \right)^2}{1 - \left(\frac{h}{Na} \right)^2} \right] \frac{\mathbf{h} \otimes \mathbf{h}}{h^2} \quad (10)$$

$$\mathbf{A}(\mathbf{h}) \equiv \frac{2(h/Na)^2}{3 - (h/Na)^2} \frac{\mathbf{h} \otimes \mathbf{h}}{h^2} \quad (11)$$

In the Padè approximation, the single-chain characteristics (elastic free energy, stress, and orientation tensors) are also expressed in terms of chain extension h/Na .

A system of polymer chains

The closed form Eqs. (9) - (11) can be used for modelling the thermodynamic and stress-orientation properties of flexible-chain polymers in the entire range of chain extensions. Averaging of the individual chain characteristics requires a distribution of the chain end-to-end vectors, appropriate for the system and the applied deformation. The average free energy, stress, and orientation tensors are given by the integrals

$$\langle F_{el} \rangle = \iiint F_{el}(\mathbf{h}) W(\mathbf{h}) d^3 \mathbf{h} \quad (12)$$

$$\langle \mathbf{p} \rangle = \iiint \mathbf{p}(\mathbf{h}) W(\mathbf{h}) d^3 \mathbf{h} \quad (13)$$

$$\langle \mathbf{A} \rangle = \iiint \mathbf{A}(\mathbf{h}) W(\mathbf{h}) d^3 \mathbf{h} \quad (14)$$

where $W(\mathbf{h})$ is the distribution function of the chain end-to-end vectors in the deformed system. Control of the distribution is different in a solid and in a fluid state.

In an uncrosslinked system subjected to flow deformation, time evolution of the distribution is given by the continuity equation

$$\frac{\partial W}{\partial t} + \text{div} \left[W \mathbf{Q} \mathbf{h} - D \left(\nabla W + W \nabla \frac{F_{el}}{kT} \right) \right] = 0 \quad (15)$$

where D is the relative diffusion coefficient of the chain ends. The divergence and gradient operators concern the \mathbf{h} -space. \mathbf{Q} , the deformation rate tensor of the imposed flow, is purely extensional

$$\mathbf{Q} = \nabla \mathbf{V} = \begin{bmatrix} q_1 & 0 & 0 \\ 0 & q_2 & 0 \\ 0 & 0 & q_3 \end{bmatrix} \quad (16)$$

where the axial components q_i are the axial velocity gradients.

For an isochoric flow we have $q_1 + q_2 + q_3 = 0$. Distribution $W(\mathbf{h}, t)$ is affected by the flow convection with velocity $\mathbf{Q} \mathbf{h}$, by the retractive elastic force between the chain ends, and by the thermal motion of chain ends. Each chain can be represented by a Brownian, non-linearly elastic dumbbell subjected to the extensional flow.

In the solid state, we deal with molecular mobility very much limited by strong inter-molecular interactions, which create a sort of plastic medium with very high viscosity and the chain diffusion coefficient practically reduced to zero. In the limit of zero diffusion coefficient, $D \rightarrow 0$, and finite elastic free energy of the individual chains, Eq. (15) reduces to a first order differential evolution equation

$$\frac{\partial W}{\partial t} + W \text{tr} \mathbf{Q} + (\mathbf{Q} \mathbf{h}) \cdot \nabla W = 0 \quad (17)$$

The solution of the equation, with an initial distribution $W_0(\mathbf{h})$, corresponds to the distribution at affine deformation of \mathbf{h} vectors with time-dependent displacement gradient tensor

$$\mathbf{\Lambda}(t) = \begin{bmatrix} \lambda_1(t) & 0 & 0 \\ 0 & \lambda_2(t) & 0 \\ 0 & 0 & \lambda_3(t) \end{bmatrix} \quad (18)$$

where $\lambda_i(t) = \exp(q_i t)$, and reads

$$W(\mathbf{h}, t) = W_0[\mathbf{\Lambda}(t)\mathbf{h}] / \det \mathbf{\Lambda}(t) \quad (19)$$

For isochoric flow we have $\det \mathbf{\Lambda}(t) = 1$.

Considering a Boltzmann initial distribution, controlled by the non-Gaussian elastic free energy, we obtain

$$W(\mathbf{h}, t) = C [\det \mathbf{\Gamma}(t)]^{-1/2} \exp \left[-N \int_0^{(\mathbf{h}\mathbf{\Gamma}^{-1}\mathbf{h})^{1/2}/Na} L^*(x) dx \right] \quad (20)$$

C is a normalisation constant, and $\mathbf{\Gamma}$ the time-dependent deformation tensor

$$\mathbf{\Gamma}(t) = \mathbf{\Lambda}^T(t)\mathbf{\Lambda}(t) = \begin{bmatrix} \lambda_1^2 & 0 & 0 \\ 0 & \lambda_2^2 & 0 \\ 0 & 0 & \lambda_3^2 \end{bmatrix} \quad (21)$$

Distribution (20) is typical of affine deformations of crosslinked polymers, as well. We use the distribution to discuss biaxial affine deformation of polymer solids, uncross-linked or rubbery networks.

With the Padè approximation, the affine distribution for isochoric deformation ($\det \mathbf{\Gamma} = 1$) reads

$$W(\mathbf{h}) \cong C \left(1 - \frac{\mathbf{h} \cdot \mathbf{\Gamma}^{-1} \mathbf{h}}{N^2 a^2} \right)^N \exp \left(-\frac{1}{2} \frac{\mathbf{h} \cdot \mathbf{\Gamma}^{-1} \mathbf{h}}{Na^2} \right) \quad (22)$$

For small deformations, distributions (20) and (22) reduce to the Gaussian form

$$W(\mathbf{h}) = \left(\frac{3}{2\pi Na^2} \right)^{3/2} \exp \left(-\frac{3}{2} \frac{\mathbf{h} \cdot \mathbf{\Gamma}^{-1} \mathbf{h}}{Na^2} \right) \quad (23)$$

In a fluid system we deal with higher values of the diffusion constant. Two asymptotic solutions of the continuity Eq. (15) are obtained. In the limit of infinite diffusion constant, $D \rightarrow \infty$, and relatively small rates of flow deformation, when \mathbf{Q}/D can be neglected, the distribution approaches equilibrium Boltzmann distribution controlled by the chain elastic free energy

$$W(\mathbf{h}) = C \exp \left[-N \int_0^{h/Na} L^*(x) dx \right] \quad (24)$$

Flow effects do not appear in the distribution. In this case we cannot produce effective segmental orientation by the flow.

The flow deformation should be effective for segmental orientation if the reduced deformation rate tensor \mathbf{Q}/D cannot be neglected at finite diffusion rate, i.e., at relatively fast flow rates. Symmetry of the tensor \mathbf{Q} determines symmetry of the produced molecular orientation.

Steady-state distribution of \mathbf{h} vectors under such conditions assumes an equilibrium Boltzmann form [20] controlled by a potential being a sum of the elastic free energy

$F_{el}(\mathbf{h})$ and a flow potential $kTh \cdot (\mathbf{Q}/D)\mathbf{h}/2$. Introducing a relaxation time inversely proportional to the diffusion coefficient, $\tau = Na^2/6D$, the equilibrium distribution for the flow reads

$$W(\mathbf{h}) = C \exp \left[-N \int_0^{h/Na} L^*(x) dx + \frac{3\tau}{Na^2} \mathbf{h} \cdot \mathbf{Q}\mathbf{h} \right] \quad (25)$$

With the Padé approximation, the distribution assumes the following form

$$W(\mathbf{h}) \cong C \left(1 - \frac{h^2}{N^2 a^2} \right)^N \exp \left(-\frac{1}{2} \frac{h^2}{Na^2} + \frac{3\tau}{Na^2} \mathbf{h} \cdot \mathbf{Q}\mathbf{h} \right) \quad (26)$$

At small $\tau\mathbf{Q}$, distributions (25) and (26) reduce to the flow-modified Gaussian form

$$W(\mathbf{h}) = C \exp \left[-\frac{3}{2} \frac{\mathbf{h} \cdot (\mathbf{I} - 2\tau\mathbf{Q})\mathbf{h}}{Na^2} \right] \quad (27)$$

Below we discuss segmental orientation and stresses in biaxial affine deformation of uncrosslinked polymer solids and rubbery networks, as well as in biaxial extensional flow of chains in a viscous liquid, obtained using the above model.

Affine deformation in the solid state

We consider an affine, biaxial stretching of the polymer chains along horizontal x_1 and zenithal x_3 axes of an external system of co-ordinates, with the stretch ratios λ_1 and λ_3 , respectively. The remaining horizontal stretch ratio λ_2 results as $1/\lambda_1\lambda_3$ from the condition of isochoric deformation. Then, the macroscopic and molecular deformation tensors are equal and read

$$\mathbf{\Gamma} = \begin{bmatrix} \lambda_1^2 & 0 & 0 \\ 0 & 1/\lambda_1^2\lambda_3^2 & 0 \\ 0 & 0 & \lambda_3^2 \end{bmatrix} \quad (28)$$

The initial distribution of end-to-end vectors is assumed to be an equilibrium, non-Gaussian distribution, controlled by the inverse Langevin elastic free energy. In the uniaxial case, the stretch ratios reduce to $\lambda_1 = \lambda_2 = 1/\lambda_3^{1/2}$.

Using the non-Gaussian distribution function, Eq. (20), the average elastic free energy, stress and orientation tensors in the series expansion form read

$$\frac{\langle F_{el} \rangle}{NkT} = \frac{1}{2} \text{tr} \left(\frac{\mathbf{\Gamma}}{N} \right) + \frac{1}{20} \left[2 \text{tr} \left(\frac{\mathbf{\Gamma}}{N} \right)^2 + \left(\text{tr} \left(\frac{\mathbf{\Gamma}}{N} \right) \right)^2 \right] + O \left(\left(\frac{\mathbf{\Gamma}}{N} \right)^3 \right) \quad (29)$$

$$\frac{\langle \mathbf{p} \rangle \cdot \mathbf{v}_0}{kT} = \frac{\mathbf{\Gamma}}{N} + \frac{1}{5} \left[2 \left(\frac{\mathbf{\Gamma}}{N} \right)^2 + \frac{\mathbf{\Gamma}}{N} \text{tr} \left(\frac{\mathbf{\Gamma}}{N} \right) \right] + O \left(\left(\frac{\mathbf{\Gamma}}{N} \right)^3 \right) \quad (30)$$

$$\langle \mathbf{A} \rangle = \frac{1}{5} \frac{\mathbf{\Gamma}}{N} + \frac{4}{175} \left[2 \left(\frac{\mathbf{\Gamma}}{N} \right)^2 + \frac{\mathbf{\Gamma}}{N} \text{tr} \left(\frac{\mathbf{\Gamma}}{N} \right) \right] + O \left(\left(\frac{\mathbf{\Gamma}}{N} \right)^3 \right) \quad (31)$$

The average characteristics depend on the macroscopic deformation tensor reduced by the number of statistical segments in the chain, $\mathbf{\Gamma}/N$. Components of the reduced deformation tensor characterise an effective molecular deformation. The first term in each average, linear in $\mathbf{\Gamma}/N$, corresponds to Gaussian statistics and leads to the well known linear stress-orientation law

$$\langle \mathbf{A} \rangle = \frac{1}{5} \frac{\langle \mathbf{p} \rangle \cdot \mathbf{v}_0}{kT} \quad (32)$$

The average axial orientation of chain segments is usually characterised by the axial orientation factor, an average of the second order Legendre polynomial of cosine of the angle between the segment and the deformation axis. Axial orientation factors f_1 , f_2 , f_3 characterise orientations with respect to the co-ordinates' axes, and are given by the components of the deviator of the average orientation tensor

$$\mathbf{D} \equiv \langle \mathbf{A} \rangle - \frac{1}{3} \text{tr} \langle \mathbf{A} \rangle \mathbf{I} = \frac{2}{3} \begin{bmatrix} f_1 & 0 & 0 \\ 0 & f_2 & 0 \\ 0 & 0 & f_3 \end{bmatrix} \quad (33)$$

The axial orientation factors read

$$\begin{aligned} f_1 &= \langle A_{11} \rangle - \frac{1}{2} (\langle A_{22} \rangle + \langle A_{33} \rangle) \\ f_2 &= \langle A_{22} \rangle - \frac{1}{2} (\langle A_{11} \rangle + \langle A_{33} \rangle) \\ f_3 &= \langle A_{33} \rangle - \frac{1}{2} (\langle A_{11} \rangle + \langle A_{22} \rangle) \end{aligned} \quad (34)$$

where $\langle A_{ij} \rangle$ are components of the average orientation tensor, Eq. (14).

We note that the sum $f_1 + f_2 + f_3 = 0$.

The norm of the tensor \mathbf{D}

$$\|\mathbf{D}\| = [\text{tr}(\mathbf{D}\mathbf{D}^T)]^{1/2} = \frac{2}{3} (f_1^2 + f_2^2 + f_3^2)^{1/2} \quad (35)$$

is a scalar characteristic of the system global anisotropy.

Using the expansion form of the average orientation tensor we obtain

$$f_1 = \frac{1}{5N} \left[\lambda_1^2 - \frac{1}{2} \left(\lambda_3^2 + \frac{1}{\lambda_1^2 \lambda_3^2} \right) \right] + \quad (36)$$

$$+ \frac{8}{175N^2} \left\{ \lambda_1^4 - \frac{1}{2} \left(\lambda_3^4 + \frac{1}{\lambda_1^4 \lambda_3^4} \right) + \frac{1}{2} \left(\lambda_1^2 + \lambda_3^2 + \frac{1}{\lambda_1^2 \lambda_3^2} \right) \left[\lambda_1^2 - \frac{1}{2} \left(\lambda_3^2 + \frac{1}{\lambda_1^2 \lambda_3^2} \right) \right] \right\} + \mathcal{O}\left(\frac{1}{N^3}\right)$$

$$f_3 = \frac{1}{5N} \left[\lambda_3^2 - \frac{1}{2} \left(\lambda_1^2 + \frac{1}{\lambda_1^2 \lambda_3^2} \right) \right] + \quad (37)$$

$$+ \frac{8}{175N^2} \left\{ \lambda_3^4 - \frac{1}{2} \left(\lambda_1^4 + \frac{1}{\lambda_1^4 \lambda_3^4} \right) + \frac{1}{2} \left(\lambda_1^2 + \lambda_3^2 + \frac{1}{\lambda_1^2 \lambda_3^2} \right) \left[\lambda_3^2 - \frac{1}{2} \left(\lambda_1^2 + \frac{1}{\lambda_1^2 \lambda_3^2} \right) \right] \right\} + \mathcal{O}\left(\frac{1}{N^3}\right)$$

$$f_2 = -(f_1 + f_3) \quad (38)$$

First terms in the above expressions correspond to the Gaussian chain statistics.

For the uniaxial case, the orientation factors reduce to

$$f_3 = \frac{1}{5N} \left(\lambda_3^2 - \frac{1}{\lambda_3} \right) + \frac{4}{175N^2} \left(3\lambda_3^4 + \lambda_3 - \frac{4}{\lambda_3} \right) + \mathcal{O}\left(\frac{1}{N^3}\right) \quad (39)$$

$$f_1 = f_2 = -\frac{1}{2} f_3 \quad (40)$$

The series-expansion approach leads to weakly convergent expressions, in particular at higher - biaxial or uniaxial - deformations.

We average the individual chain characteristics with the affine, non-Gaussian distribution of \mathbf{h} vectors in the Padè approximation, Eq. (22). Solid lines in Fig. 2 and Fig. 3 illustrate the axial orientation factors f_1 and f_3 vs. transversal stretch ratio λ_3 , at fixed

axial stretch ratio λ_1 (indicated), computed with the Padè approximation of the non-Gaussian distribution. Stretch ratios smaller than unity correspond to compression. The stretch range is limited by full extension of an average chain conformation, i.e., the one with end-to-end distance equal to $N^{1/2}a$ in the undeformed state. We assume the number of statistical segments in each chain $N = 100$, and our computations apply to

$$\lambda_1^2 + \lambda_3^2 + 1/(\lambda_1\lambda_3)^2 < N \quad (41)$$

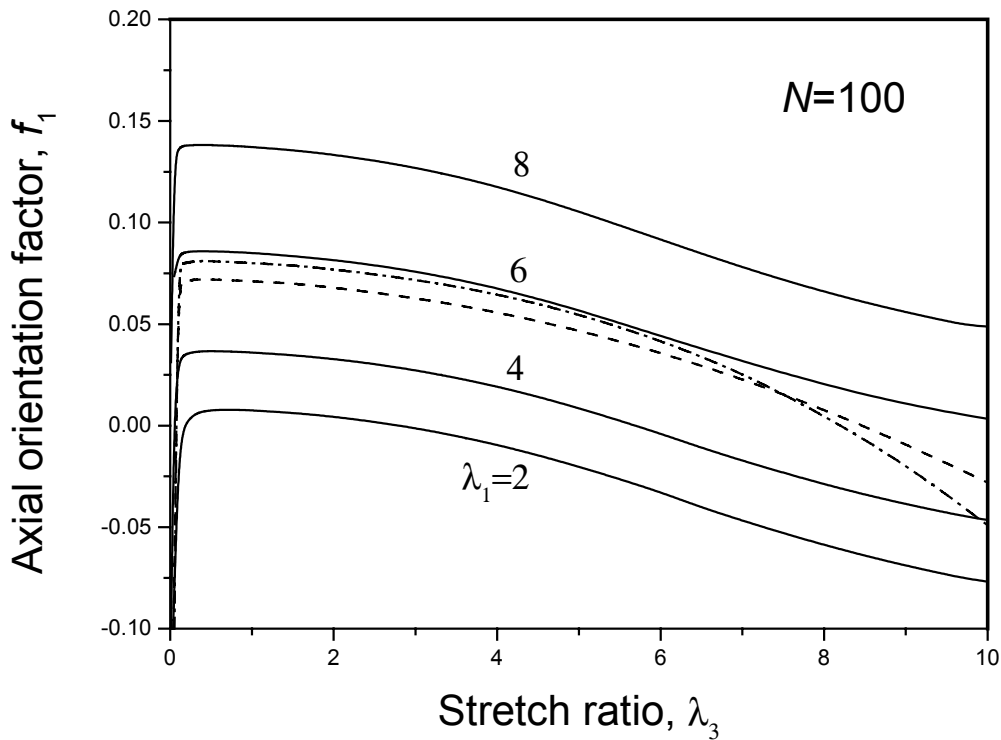


Fig. 2. Axial orientation factor f_1 vs. transversal stretch ratio λ_3 at fixed stretch ratio λ_1 (indicated) for affine biaxial deformation of non-Gaussian chains in the Padè approximation (solid lines), computed from Eqs. (11) and (22). Dashed line – computed from the Gaussian term in Eq. (36), dash-dotted line – from two terms of the series expansion, Eq. (36), at $\lambda_1 = 6$

As expected, transversal stretch reduces the axial orientation factor f_1 (Fig. 2) monotonically with increasing transversal stretch ratio λ_3 . A negative axial orientation factor indicates domination of transversal orientation of chain segments. The orientation is produced by dominating transversal stretch, or by compression. The orientation factor f_3 can be enhanced by a co-axial stretch, and it increases monotonically with stretch ratio λ_3 .

Example deviations of the Gaussian model, Eq. (36), and the two-term series expansion model, Eq. (37), are illustrated, respectively, by the dashed and dash-dotted lines in the figures. The two-term model gives results being closer to the model with Padè approximation, but both of them significantly deviate at higher deformations.

Our results can be compared with the results of a series expansion theory based on the Nagai formulation [21] of segmental orientation, and obtained by Sarac et al. [13] The slopes of the plots shown in Fig. 2 and Fig. 3 show stronger effects of stretch,

say λ_3 , on the co-axial orientation factor, f_3 , than on f_1 . A similar conclusion for infinitesimally small deformations was found in the series expansion model [13]. Tendencies of the segmental orientation behaviour in biaxial affine deformation predicted in our approach and by the series expansion model [13] are in qualitative agreement. However, the results shown in ref. [13] are limited to second-order approximation, and indicate significant differences between the first- and second-order approximations at higher stretch ratios. This source of uncertainty is reduced in the closed-form approximation of the inverse Langevin statistics.

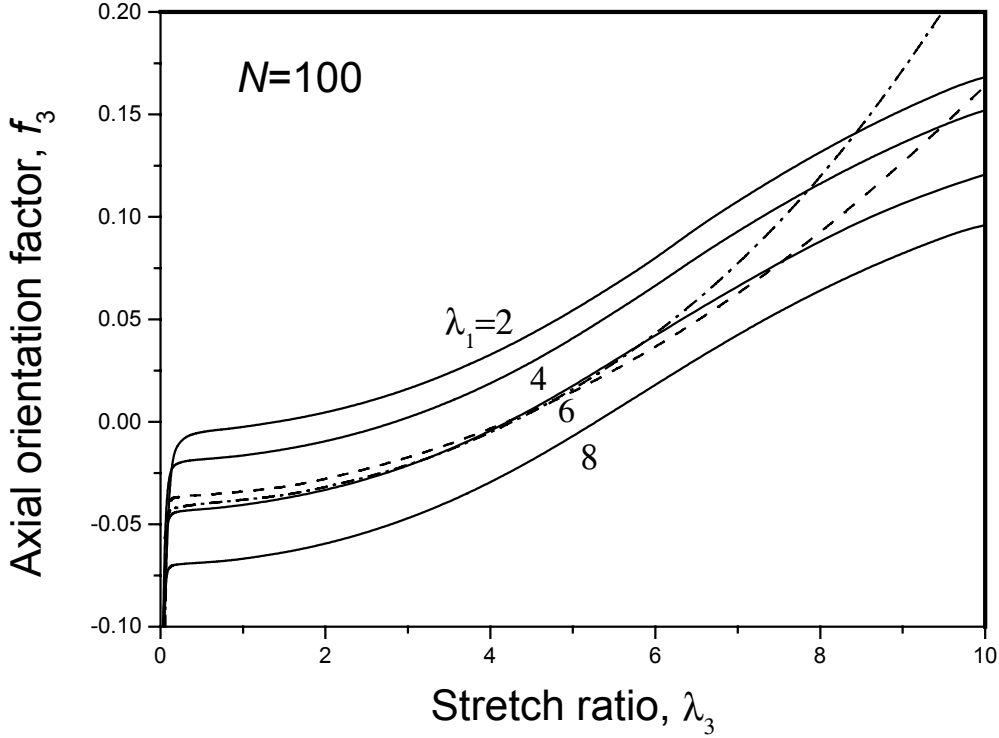


Fig. 3. Axial orientation factor f_3 vs. stretch ratio λ_3 at fixed stretch ratio λ_1 (indicated) for affine biaxial deformation of non-Gaussian chains in the Padé approximation (solid lines), computed from Eqs. (11) and (22). Dashed line – computed from the Gaussian term in Eq. (37), dash-dotted line – from two terms of the series expansion, Eq. (37), at $\lambda_1 = 6$

The average normal stress differences in the series-expansion approach read

$$\langle p_{33} \rangle - \langle p_{11} \rangle = \frac{kT}{Nv_0} (\lambda_3^2 - \lambda_1^2) + \frac{1}{5} \frac{kT}{N^2 v_0} \left(3\lambda_3^4 - \frac{1}{\lambda_3^2} - 3\lambda_1^4 + \frac{1}{\lambda_1^2} \right) + O\left(\frac{1}{N^3}\right) \quad (42)$$

$$\langle p_{33} \rangle - \langle p_{22} \rangle = \frac{kT}{Nv_0} \left(\lambda_3^2 - \frac{1}{\lambda_1^2 \lambda_3^2} \right) + \frac{1}{5} \frac{kT}{N^2 v_0} \left(3\lambda_3^4 - \frac{3}{\lambda_1^4 \lambda_3^4} + \lambda_1^2 \lambda_3^2 - \frac{1}{\lambda_3^2} \right) + O\left(\frac{1}{N^3}\right) \quad (43)$$

For the uniaxial case, the above formulae reduce to

$$\langle p_{33} \rangle - \langle p_{11} \rangle = \frac{kT}{Nv_0} \left(\lambda_3^2 - \frac{1}{\lambda_3} \right) + \frac{1}{5} \frac{kT}{N^2 v_0} \left(3\lambda_3^4 + \lambda_3 - \frac{4}{\lambda_3} \right) + O\left(\frac{1}{N^3}\right) \quad (44)$$

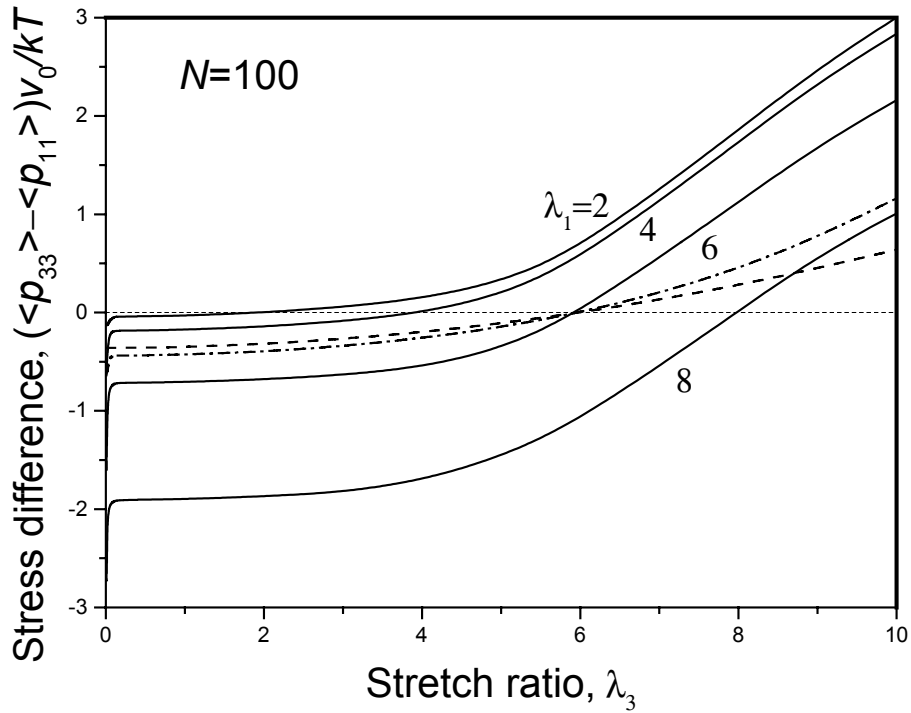


Fig. 4. Reduced normal stress difference $(\langle p_{33} \rangle - \langle p_{11} \rangle)v_0/kT$ vs. stretch ratio λ_3 at fixed λ_1 (indicated) for affine biaxial deformation of non-Gaussian chains in the Padé approximation (solid lines), computed from Eqs. (10) and (22). Dashed line – computed from the Gaussian term in Eq. (42), dash-dotted line – from two terms of the series expansion, Eq. (42), at $\lambda_1 = 6$

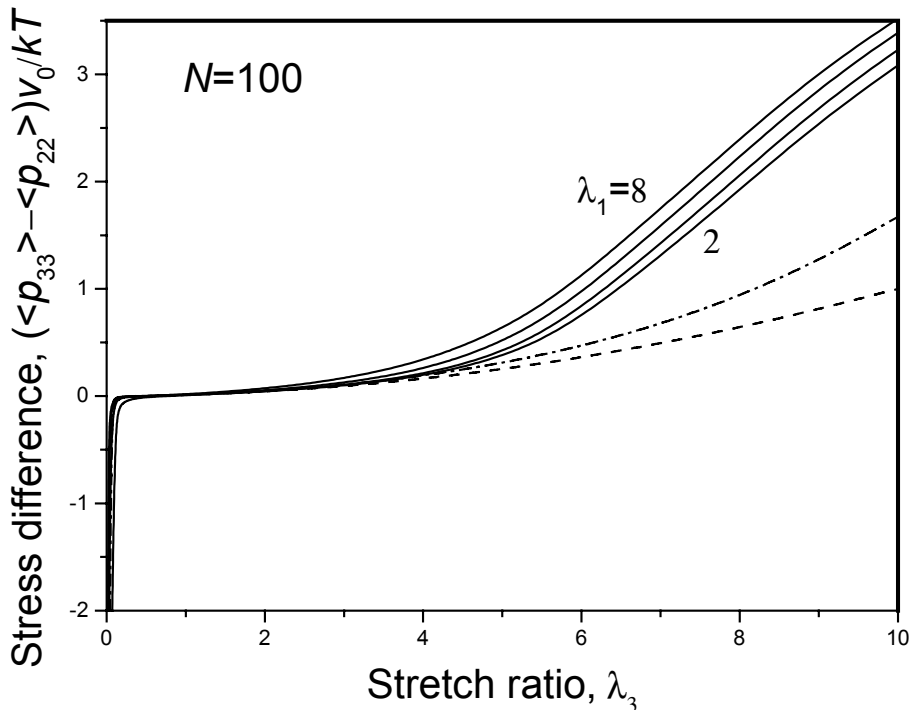


Fig. 5. Reduced normal stress difference $(\langle p_{33} \rangle - \langle p_{22} \rangle)v_0/kT$ vs. stretch ratio λ_3 at fixed $\lambda_1 = 2, 4, 6,$ and 8 for affine biaxial deformation of non-Gaussian chains in the Padé approximation (solid lines), computed from Eqs. (10) and (22). Dashed line – computed from the Gaussian term in Eq. (43), dash-dotted line – from two terms of the series expansion, Eq. (43), at $\lambda_1 = 6$

Fig. 4 and Fig. 5 show reduced average normal stress differences, $(\langle p_{33} - \langle p_{11} \rangle \rangle) v_0 / kT$ and $(\langle p_{33} \rangle - \langle p_{22} \rangle) v_0 / kT$, respectively, vs. stretch ratio λ_3 at fixed values of λ_1 (indicated). Solid lines, computed for the non-Gaussian chain statistics with the Padè approximation, monotonically increase with increasing stretch ratios. The stress difference in the deformation plane, $\langle p_{33} \rangle - \langle p_{11} \rangle$, is higher than that in the normal plane, $\langle p_{33} \rangle - \langle p_{22} \rangle$. Steeper increase of $\langle p_{33} \rangle - \langle p_{11} \rangle$ in the deformation plane with increasing transversal stretch is predicted for transversal stretch ratios λ_3 exceeding λ_1 .

Example deviations of the single-term (Gaussian) and two-term approximations are illustrated in the figures by dashed lines. Both approximations, the Gaussian and the two-term approximation, predict a milder increase of the stress differences than the closed-formula, Padè approximation. Deviations of both models from the Padè approximation are much higher at higher deformations.

Flow deformation

We consider deformation and orientation of polymer chains in a viscous fluid subjected to biaxial extensional flow, co-axial with horizontal x_1 and vertical x_3 axes of an external co-ordinate system. The extensional flow field is uniform, with a velocity gradient tensor, or deformation rate tensor, in the form

$$\mathbf{Q} = \begin{bmatrix} q_1 & 0 & 0 \\ 0 & -(q_1 + q_3) & 0 \\ 0 & 0 & q_3 \end{bmatrix} \quad (45)$$

where q_1 and q_3 are axial velocity gradients, or axial elongation rates. Velocity gradient q_2 for isochoric flow deformation is determined from the condition $\text{tr } \mathbf{Q} = q_1 + q_2 + q_3 = 0$. For the uniaxial case we have $q_1 = q_2 = -q_3/2$.

For Gaussian chain statistics, valid for small elongation rates $\tau q_i \ll 1/2$, flow distribution of the chain end-to-end vectors, Eq. (27), leads to the average characteristics

$$\frac{\langle F_{el} \rangle}{NkT} = \frac{1}{2} \text{tr} \left(\frac{\Gamma_H}{N} \right) \quad (46)$$

$$\frac{\langle \mathbf{p} \rangle v_0}{kT} = \frac{\Gamma_H}{N} \quad (47)$$

$$\langle \mathbf{A} \rangle = \frac{1}{5} \frac{\Gamma_H}{N} \quad (48)$$

The tensor

$$\Gamma_H = (\mathbf{I} - 2\tau\mathbf{Q})^{-1} = \begin{bmatrix} 1/(1-2\tau q_1) & 0 & 0 \\ 0 & 1/[1+2\tau(q_1+q_3)] & 0 \\ 0 & 0 & 1/(1-2\tau q_3) \end{bmatrix} \quad (49)$$

characterises molecular deformation of the Gaussian chains in the flow. The tensor Γ_H shows a singularity at the reduced elongation rates $\tau q_1 = 1/2$ and/or $\tau q_3 = 1/2$, at which the flow potential compensates the elastic free energy of the Gaussian chains. The Gaussian-type averages (46) - (48) are identical with those obtained for affine deformation, but with the deformation tensor Γ replaced by Γ_H . Similarly, effects of flow deformation are controlled by the molecular deformation tensor reduced by the number of statistical segments in a chain, Γ_H/N .

Molecular deformation in the flow is controlled by the product of macroscopic elongation rate and relaxation time, τq_i , reflecting the role of viscous interactions between the chains and the flowing medium.

For Gaussian chains, the axial orientation factors are expressed in terms of the components of the molecular deformation tensor, $1/(1-2\tau q_i)$, and read

$$f_1 = \frac{1}{5N} \left[\frac{1}{1-2\tau q_1} - \frac{1}{2} \left(\frac{1}{1-2\tau q_3} + \frac{1}{1+2\tau(q_1+q_3)} \right) \right] \quad (50)$$

$$f_3 = \frac{1}{5N} \left[\frac{1}{1-2\tau q_3} - \frac{1}{2} \left(\frac{1}{1-2\tau q_1} + \frac{1}{1+2\tau(q_1+q_3)} \right) \right] \quad (51)$$

For the case of uniaxial elongational flow, along the x_3 axis, the orientation factors reduce to

$$f_3 = \frac{3}{5N} \frac{\tau q_3}{1-\tau q_3(1+2\tau q_3)}, \quad f_1 = f_2 = -\frac{1}{2} f_3 \quad (52)$$

At higher elongation rates, the system deviates from Gaussian, and no longer such an affine-type molecular deformation represented by tensor Γ_H takes place.

Orientalional behaviour at higher elongation rates can be discussed using inverse Langevin flow distribution of the chain end-to-end vectors with the Padè approximation, Eq. (26). This formula is tractable in the entire range of flow intensities. Axial orientation factors f_1 and f_3 computed with the non-Gaussian distribution are shown in Fig. 6 and Fig. 7 vs. elongation rate τq_3 , at fixed τq_1 values. The number of statistical segments in a chain is fixed to $N = 100$.

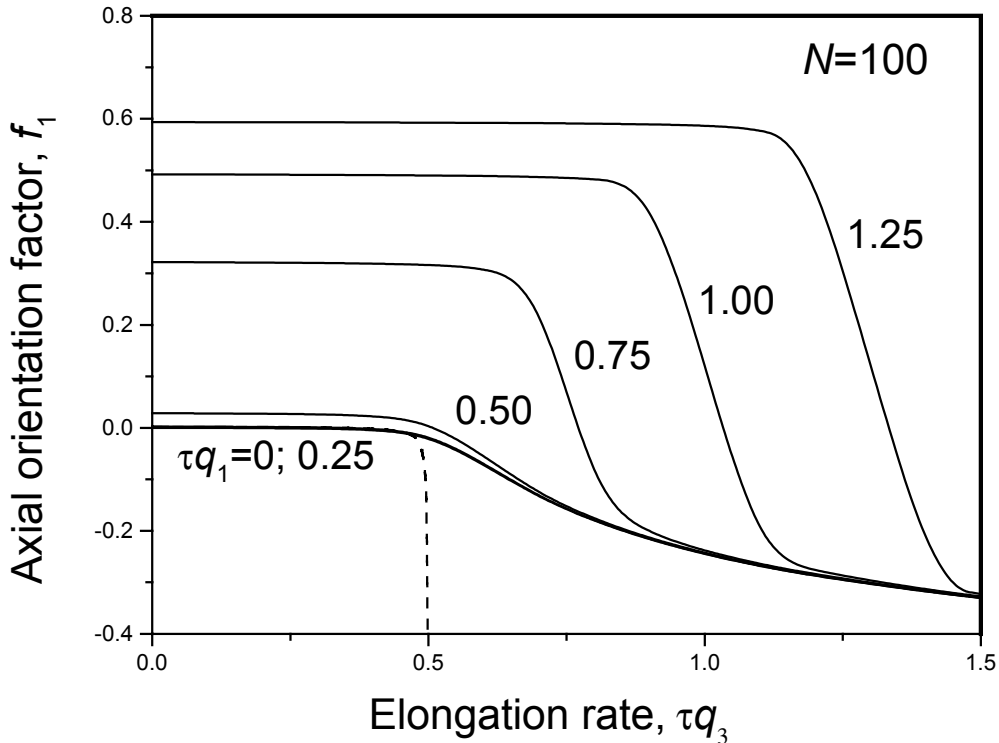


Fig. 6. Axial orientation factor f_1 vs. reduced transversal elongation rate τq_3 , at fixed values of τq_1 (indicated), computed for biaxial flow deformation of non-Gaussian chains in a viscous fluid with the flow distribution in Padè approximation, Eq. (26). Dashed line – Gaussian chains at $\tau q_1 = 0.25$; note the singularity at $\tau q_3 = 0.5$

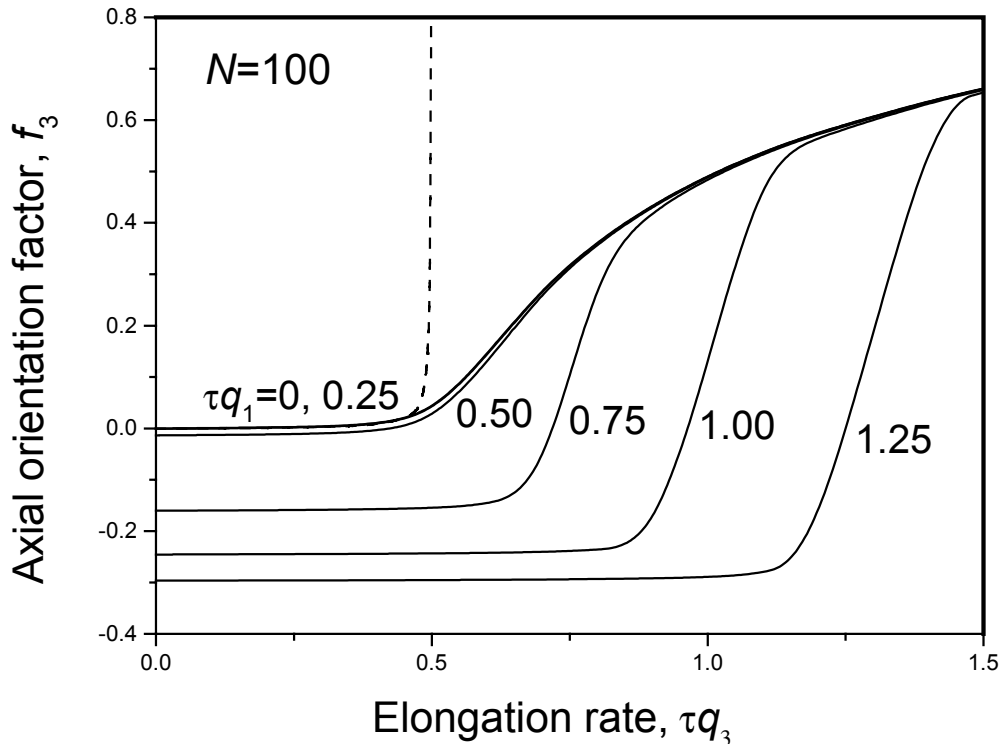


Fig. 7. Axial orientation factor f_3 vs. reduced elongation rate τq_3 , at fixed values of τq_1 (indicated), computed for biaxial flow deformation of non-Gaussian chains in a viscous fluid with the flow distribution in Padè approximation. Lines like in Fig. 6

Orientation factors computed from the non-Gaussian model with the Padè approximation do not show any singularity. A singularity appears for the system of Gaussian chains at $\tau q_1 = 0.5$ or $\tau q_3 = 0.5$. At flow rates τq_1 or τq_3 exceeding 0.5, the distribution of end-to-end vectors in the Gaussian system is undefined. This is a well known feature of Gaussian systems. Examples of such behaviour are illustrated in Fig. 6 and Fig. 7 by dashed lines, computed from Eqs. (50) and (51), respectively, at fixed $\tau q_1 = 0.25$.

Similarly to affine biaxial deformation in solids, transversal flow reduces axial orientation, and the effect takes place in the range of transversal flow intensities, τq_3 , comparable with those of the co-axial flow, within a range of about ± 0.25 . Transversal flows with intensities below that range do not affect axial orientation, and the plots show a plateau in Fig. 6, the wider the higher the co-axial elongation rate. Each plateau is followed by a steep reduction of the axial orientation factor to negative values, which next converges to a common asymptote at high transversal elongation rates, indicating high transversal orientation. The behaviour concerns reduced elongation rates, co-axial or transversal, exceeding the value of 0.5.

Simultaneously, axial orientation in the transversal direction is built up and converges to a common asymptote of high orientation at high flow rates, as illustrated in Fig. 7. The common asymptote, as well as the wide plateau of the orientation factor at lower transversal deformation rates, are not predicted in the case of affine deformation in polymer solids.

At lower elongation rates, segmental orientation is very weak, and the orientation factors do not exceed 0.03 for the co-axial and -0.015 for the transversal orientation. The transition to the regime of high orientation takes place at reduced elongation rates of about 0.5, where the Gaussian model shows a singularity and becomes

intractable. Then, the discussion of high segmental orientation produced in the extensional flow is possible with the application of non-Gaussian chain statistics. Here we use the Padè approximation of the distribution.

The normal stress differences calculated in the Gaussian approximation read

$$\langle p_{33} \rangle - \langle p_{11} \rangle = \frac{kT}{Nv_0} \left(\frac{1}{1-2\tau q_3} - \frac{1}{1-2\tau q_1} \right) \quad (53)$$

$$\langle p_{33} \rangle - \langle p_{22} \rangle = \frac{kT}{Nv_0} \left(\frac{1}{1-2\tau q_3} - \frac{1}{1+2\tau(q_1+q_3)} \right) \quad (54)$$

For the uniaxial case, the stress differences in the Gaussian approximation reduce to

$$\langle p_{33} \rangle - \langle p_{11} \rangle = \langle p_{33} \rangle - \langle p_{22} \rangle = \frac{3kT}{Nv_0} \frac{\tau q_3}{1-\tau q_3(1+2\tau q_3)} \quad (55)$$

The reduced normal stress differences $(\langle p_{33} \rangle - \langle p_{11} \rangle)v_0/kT$ and $(\langle p_{33} \rangle - \langle p_{22} \rangle)v_0/kT$, computed with the non-Gaussian distribution and the Padè approximation, are plotted in Fig. 8 and Fig. 9 vs. τq_3 , at fixed values of τq_1 . The dashed-lines show the stresses computed from the Gaussian model. The stress differences show a plateau in the range of the transversal elongation rates τq_3 lower than τq_1 . Similarly to the axial orientation, the stress differences increase steeply in the range where both elongation rates τq_1 and τq_3 are comparable to each another, within a range of about ± 0.25 . Next, they approach a common asymptote at higher deformation rates. The steep increase is followed by a mildly increasing common asymptote. The effective increase in segmental orientation takes place at the reduced elongation rates exceeding 0.5, where the Gaussian model is unphysical. At the reduced elongation rates below 0.5, both stress differences are very low, similarly to the axial orientation factors.

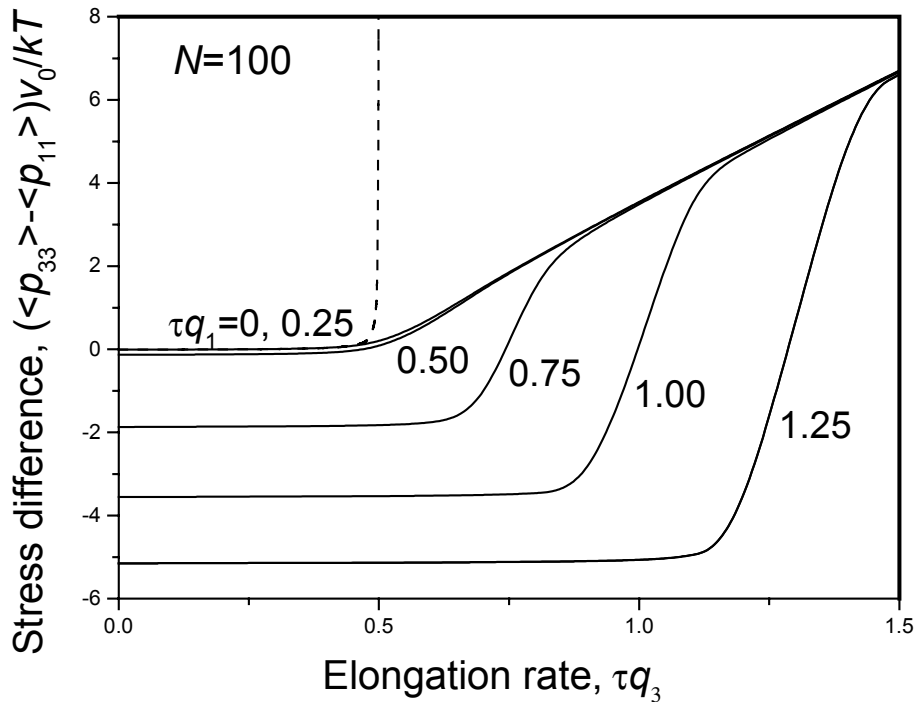


Fig. 8. Reduced normal stress difference $(\langle p_{33} \rangle - \langle p_{11} \rangle)v_0/kT$ vs. reduced transversal elongation rate τq_3 , at fixed values of τq_1 (indicated), computed for biaxial elongational flow of non-Gaussian chains in a viscous fluid with the flow distribution in Padè approximation. Lines like in Fig. 6

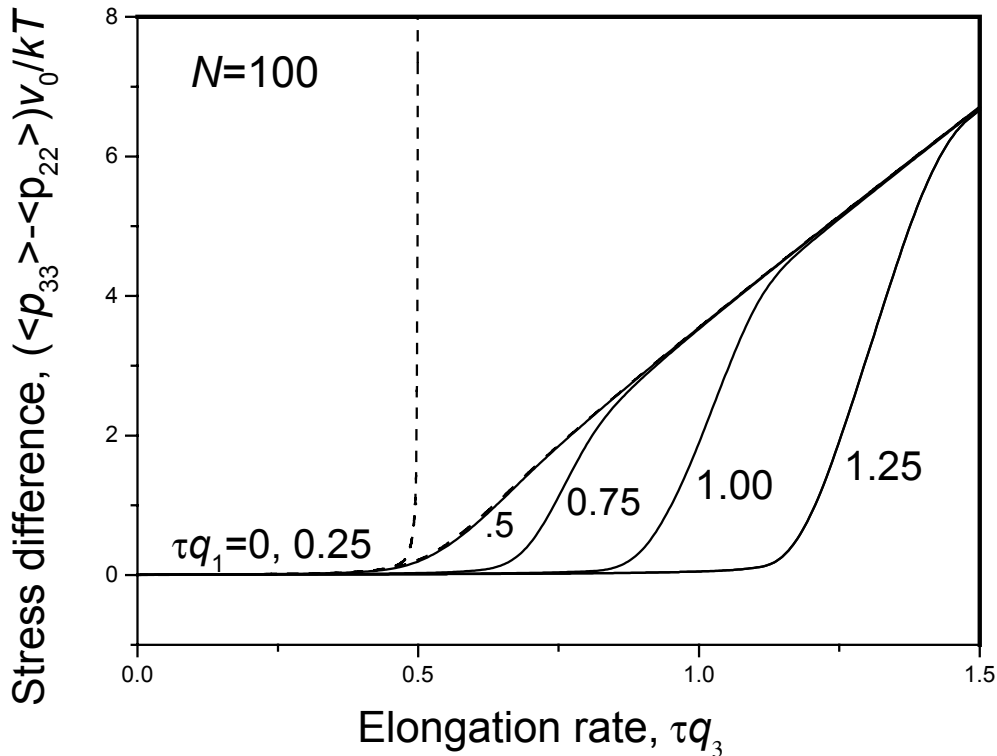


Fig. 9. Reduced normal stress difference $(\langle p_{33} \rangle - \langle p_{22} \rangle)v_0/kT$ vs. reduced elongation rate τq_3 , at fixed values of τq_1 (indicated), computed for biaxial flow deformation of non-Gaussian chains in a viscous fluid with the flow distribution in Padé approximation, Eq. (26). Lines like in Fig. 6

The model concerns the effects of an intra-chain non-linear elastic potential, and related finite chain extensibility, on segmental orientation and stress in systems with fixed chain length. Excluded-volume effects are neglected for condensed systems. The effective chain length can be influenced during the deformation by inter-chain entanglements. Experimental and theoretical work shows that inter-chain interactions may influence the orientation and stress characteristics, depending on the system [22-25]. The effects of intermolecular interactions are not taken into account in our calculations. Increasing degrees of cross-linking (chemical, physical) and high chain flexibility reduce an excess of orientation and stress resulting from entanglements. Also dilution with an appropriate isotropic solvent diminishes the entanglements' effect on segmental orientation.

Conclusions

- A closed-formula model of biaxial (and uniaxial) deformation, affine or viscous flow, accounting for the effects of finite chain extensibility in the elastic potential, is proposed for the entire range of chain extensions. Chain statistics bases on the Padé approximation of the inverse Langevin function in the non-Gaussian distribution. This approximation avoids slowly convergent procedures of the series expansion formulation in discussing segmental orientation and stresses in systems subjected to high molecular deformations.

- The range of affine deformation and segmental orientation in solids is limited by the full extension of an average chain conformation in biaxial stretching which leads to the condition $\lambda_i^2/N + \lambda_j^2/N + 1/\lambda_i^2 \lambda_j^2 N < 1$. Consequence of this limitation is a rather

narrow range of segmental orientation available in biaxial stretching by the affine manner.

- The segmental orientation and stresses in biaxial affine stretching are controlled by squares of the macroscopic stretch ratios reduced by the number of statistical segments, λ_i^2/N , λ_j^2/N . In the case of flow deformation, the control variables are reduced elongation rates τq_i , τq_j , reflecting viscous interactions between polymer chains and the liquid medium subjected to the flow.
- Biaxial elongational flow is more effective for segmental orientation than affine biaxial deformation. The computations indicate that highest values of the axial orientation factor in affine deformation do not exceed 0.2 while the elongational flow produces orientation factors as high as 0.5, and higher. The monotonic increase of the orientation factors at high elongation rates indicates the possibility of production of biaxial orientation between ideal transversal ($f_i = -1/2$) and ideal longitudinal alignment ($f_i = 1$) by biaxial elongational flow. Elongation rates in the biaxial flow are unlimited in the model.
- Transversal stretching in the affine biaxial deformation reduces axial orientation more effectively when it dominates the co-axial stretch ratio. Similarly, enhancement of the axial orientation by the co-axial stretch is stronger when it exceeds the transversal stretch ratio. This is accompanied by a similar behaviour of the stress differences.
- In the flow deformation, the effects of transversal elongational flow are higher than in the affine stretching, and concentrated within a narrow range of elongation rates where both elongation rates are comparable. Transversal elongation does not influence orientation and stresses when its rate is beyond that range.
- Significant deviations of the orientation and stress characteristics from the Gaussian model are predicted at higher deformations. Gaussian chain statistics is ineffective for discussion of segmental orientation and stresses in biaxial extensional flow, because of singularities and the indefinite behaviour in the range of elongation rates effective for orientation.

Acknowledgement: This work was supported in part by Dow Chemical Co., Midland, Michigan, USA. Preliminary results were presented before at the SPE-RETEC Symposium "Orientation of Polymers", Boucherville, Canada [14].

- [1] Ziabicki, A.; in "Fundamentals of Fibre Formation", J. Wiley, **1976**, pp. 225 - 229.
- [2] Perez, G.; in "High-Speed Fiber Spinning"; Kawai, H.; Ziabicki, A.; editors; J. Wiley, **1985**, p. 333.
- [3] Kashiwagi, M.; Cunningham, A.; Manuel, A.J.; Ward, I.M.; *Polymer* **1973**, *14*, 111.
- [4] Cunningham, A.; Ward, I.M.; Willis, H.A.; Zichy, V.; *Polymer* **1974**, *15*, 749.
- [5] Jarvis, D.A.; Hutchinson, I.J.; Bower, D.I.; Ward, I.M.; *Polymer* **1980**, *21*, 41.
- [6] Ward, I.M.; *Adv. Polym. Sci.* **1985**, *66*, 81.
- [7] Bower, D.I.; Jarvis, D.A.; Ward, I.M.; *J. Polym. Sci., Polym. Phys. Ed.* **1986**, *24*, 1459.

- [8] Lapersone, P.; Tassin, J.F.; Sergot, P.; Monnerie, L.; Bourvellec, G.L.; *Polymer* **1989**, *30*, 1558.
- [9] Cakmak, M.; Kim, J.C.; *J. Appl. Polym. Sci.* **1997**, *65*, 2059.
- [10] Kim, J.C.; Cakmak, M.; Zhou, X.; *Polymer* **1998**, *39*, 4225.
- [11] Sugimoto, M.; Masubuchi, Y.; Takimoto, J.; Koyama, K.; *Macromolecules* **2001**, *32*, 6056.
- [12] White, J.L.; Spruiell, J.E.; *Polym. Eng. Sci.* **1981**, *21*, 850.
- [13] Sarac, Z.; Erman, B.; Bahar, I.; *Macromolecules* **1995**, *28*, 582.
- [14] Ziabicki, A.; Jarecki, L.; "Molecular Orientation in Biaxially Deformed Polymers", *SPE- RETEC Symposium "Orientation of Polymers"*, Boucherville, Canada, September **1998**.
- [15] Cohen, A.; *Rheol. Acta* **1991**, *30*, 270.
- [16] Kuhn, W.; Grün, F.; *Kolloid Z.* **1941**, *95*, 172, 307.
- [17] Zimm, B. H.; *J. Chem. Phys.* **1956**, *24*, 269.
- [18] Flory, P.J.; "Statistical Mechanics of Chain Molecules", chapt. 8, J. Wiley, **1969**.
- [19] Ziabicki, A.; *Proc. Vth International Congress on Rheology*, vol. III, Univ. Tokyo Press, Kyoto **1970**, p. 235.
- [20] Ziabicki, A.; Jarecki, L.; *Colloid Polym. Sci.* **1986**, *264*, 343.
- [21] Nagai, K.; *J. Chem. Phys.* **1964**, *40*, 2818.
- [22] Jarry, J.P.; Monnerie, L.; *Macromolecules* **1979**, *12*, 301.
- [23] Sotta, P.; Deloche, B.; Herz, J.; Lapp, A.; Rabadeux, J.C.; *Macromolecules* **1987**, *20*, 2769.
- [24] Erman, B.; Bahar, I.; Kloczkowski, A.; Mark, J.E.; *Macromolecules* **1990**, *23*, 5335.
- [25] Bicerano, J.; Grant, N.C.; Seitz, J.T.; Pant, K.; *J. Polym. Sci., Part B: Polym. Phys.* **1997**, *35*, 2715.